

Stochastic Geometry-Based Model for Dynamic Allocation of Metering Equipment in Spatio-Temporal Expanding Power Grids

Rachad Atat, *Member, IEEE*, Muhammad Ismail, *Senior Member, IEEE*, Mostafa F. Shaaban, *Member, IEEE*, Erchin Serpedin, *Fellow, IEEE*, and Thomas Overbye, *Fellow, IEEE*

Abstract—With smart grids replacing conventional power grids and rapidly expanding in both space and time, ensuring an acceptable system observability becomes a challenge in spatio-temporal expanding power grids. In addition, system operators face another challenge, namely, financial budget constraints. To address these challenges, a metering equipment allocation strategy for monitoring of the power grid state needs to be dynamic in both space and time. Unfortunately, existing metering allocation strategies are quite limited. They usually deal with static power grid topologies, and hence, do not reflect the spatio-temporal expansion of the power grid. In this paper, a spatio-temporal power grid model is proposed based on stochastic geometry, which we show that it is in a good match with real-world power grids. The proposed model enables us to carry out tractable dynamic allocation of metering equipment in a large (city-wide) and structurally evolving power grid. Using the developed model, a multi-year algorithm for the allocation of metering equipment is proposed based on finite horizon dynamic programming, given budgetary and technical constraints on system observability. Several case studies for metering allocation are demonstrated through simulation results.

Index Terms—Stochastic geometry, distribution system, transmission system, spatio-temporal expanding power grid, grid state uncertainty, and meter placement.

I. INTRODUCTION AND MOTIVATION

WITH power grids becoming smarter and more complex, their state of observability becomes a critical factor for optimal functionality in both operation and modes. While smart grids are expected to be in continuous expansion in both space and time dimensions, limited budget constraints impose a limit on the number of instrumentation equipment (smart meters (SMs), supervisory control and data acquisition (SCADA) metering points, energy management systems (EMSS), and phase measurement units (PMUs)) that can be installed over the deployment years [1]. This means partial observability¹

R. Atat is with the Department of Electrical and Computer Engineering, Texas A&M University at Qatar, Doha, Qatar, e-mail: rachad.atat@qatar.tamu.edu.

M. Ismail is with the Department of Computer Science, Tennessee Technological University, Cookeville, TN, 38501, USA, email: mismail@nttech.edu.

M. F. Shaaban is with the Department of Electrical and Computer Engineering, University of Waterloo, Waterloo, Canada, e-mail: mostafa.shaaban@uwaterloo.ca.

E. Serpedin and T. Overbye are with the Department of Electrical and Computer Engineering, Texas A&M University, College Station, TX, USA, email: {eserpedin,overbye}@tamu.edu.

¹A partially observable power system means that system loads and electrical elements are not fully visible or measured since metering equipment are assigned to only a subset of loads.

will be available for load allocation and estimation, voltage regulation and power loss minimization, which poses some limitation on the operation of the power grid.

To face the challenge of the partial observability of power grids, in this paper, the focus shall be on the optimal allocation of metering equipment to infer the power grid state with minimal cost, while avoiding unnecessary metering duplication. With a fixed budget that can be spent over the deployment years, system operators require a dynamic metering allocation strategy, such that in each year, an acceptable level of observability is achieved by imposing a limit on the amount of allowable uncertainty in the power grid. The uncertainty comes from the lack of accurate and sufficient data measurements, as well as from the unpredictable time-varying loads. Since the power grid is continuously expanding in both space and time, the budget should not be completely spent in the first year as the maximum allowable uncertainty in the future years might not be met. Moreover, the physical allocation of all metering equipment in the first year might not be possible as some of these metering locations might still be unavailable physically at the first year. This is the case where a metering equipment is to be allocated at a bus node that still does not physically exist in the first year. To create an efficient dynamic metering allocation strategy, a model that reflects the spatio-temporal evolution of the power grid along with a dynamic programming model for the meters placement are needed.

Unfortunately, conventional approaches suggested in the literature do not reflect the on-going changes in the complex structures of interconnected buses both in space and time. They also do not consider the mappings of the measurements of meters to their geographical locations in a city, which is an important factor to consider as electrical loads can exhibit substantial spatial correlations in a geographical area [2]. This means that the uncertainties in a power grid depend on the geographical distributions of network elements, and thus their statistics need to be taken into account.

For the scope of this paper, the focus shall be on the allocation of PMUs. Specifically, a multi-year allocation strategy that optimizes the locations of PMUs is proposed such that, in each phase of the allocation, a maximum allowable uncertainty in the power grid state is always met. For our power grid model, we use stochastic geometry, a powerful tool that allows us to describe the spatial nature of the power grid with physical buses distributed over a geographical area. Stochastic geometry also allows us to capture the temporal expansion of

the power grid, where new buses and lines are deployed in the power grid at different time steps. This eventually helps to model spatio-temporal expanding power grids as compared to static ones. Distributing buses on roads in a Poissonian city structure makes our proposed grid model more realistic and practical, since buses and metering equipment cannot be deployed in a regular fashion due to the physical constraints, as well as the energy and costs constraints [3].

Given the national security strict measures and laws in many countries, it becomes hard most of the time to obtain spatial information about the topology of the power grid. Even if topological information about the power grid was provided, most of the time it comes under strict non-disclosure agreement. This means that any related research on actual power grids cannot be shared with the research community. By using our proposed model that mimics the topological characteristics of real power grids, the developed algorithms can then be tested and applied on any actual power grid.

A. Related Work

Limited research is available on meters placement in smart grids. To improve the reliability of power quality monitoring, Ali et al. [4] used a Bayesian network-based approach and entropy-based measurements to select optimal power link locations for placing power meters such that an estimation accuracy threshold is achieved. For the data acquisition points (DAPs) placement problem, several works such as [5], [6], [7], have proposed different algorithms to optimize DAPs locations such that certain technical constraints are met. In [8], Hasan, M.M. et al. used a collaboration aware service placement for advanced metering infrastructures (AMI) buses to reduce the overall latency for monitoring upstream AMI traffic.

Different optimization models for meters placement have been proposed in literature, such as the binary semi-definite programming approach [9], the mixed-integer linear programming model [10], the mixed-integer semi-definite programming model [11], the Genetic Algorithm [12], and the convex optimization model using Fisher information matrix [13]. A graph theory approach was also proposed in [14], where a two-stage algorithm was applied to optimally place PMUs.

A mathematical model for the optimal placement of DAPs using power line communication (PLC) technology was proposed in [15]. Using queuing analysis and priority-based carrier-sensing multiple-access/collision-avoidance (CSMA/CA) scheme for scheduling delay-sensitive traffic of meters, the authors optimized the placement of DAPs such that traffic reliability with minimum installation costs are guaranteed. In [10], the authors used Benders decomposition to obtain the minimum number of micro-PMUs and SMs in microgrids to satisfy certain observability constraints at both normal steady state and contingencies state. The optimization method used allowed to reduce the computational and dimensional complexities of the suggested placement algorithm. Optimal metering placement in smart distribution grids was proposed in [13], where the authors have used Fisher information and D-optimality criterion to reduce the complexity of the developed convex optimization problem.

Using mixed-integer linear programming and the Genetic algorithm, the authors in [16] solved the optimal placement of PMUs in the presence of distributed generation (DG) units and load loss resulting from an outage. Both, DGs and maximum load loss coefficient limit were shown to affect the optimal deployment of PMUs. A mixed integer semidefinite programming model was formulated in [11] to find the optimal placement of metering equipment in distribution systems that minimizes error variances of the observability and system state estimation accuracies. In [17], the authors used an improved method of particle swarm optimization with fast convergence in order to find the minimum number of PMUs to install to ensure full system state observability. The efficiency of the results was verified on different IEEE test systems.

To the best of our knowledge, most of the research works on meters' placement either consider static traditional power distribution systems or test bus systems such as IEEE bus systems. On one hand, traditional power test systems do not reflect large power grid topological structures as they are generally much smaller in size compared with real power grids [18]. On the other hand, test power systems present a static structure; however, in reality, the topological structure of power grids is dynamic and continuously evolving as new electrical elements such as buses, lines, transformers, meters, and so on, are added to the system in addition to the seasonal reconfigurations. Moreover, the topological information becomes important to avoid redundant metering allocation since the measurements of meters can exhibit spatial correlations.

B. Contributions and Organization

The contributions of the paper are summarized as follows:

First, tools from stochastic geometry are used to model the power grid. Initially, the spatial locations of roads are modeled using a Poisson line process (PLP), and then on each road a random number of buses is generated using a homogeneous one-dimensional (1D) Poisson point process (PPP). Next, lines are constructed to connect each bus to its nearest neighbors based on geographical paths and boundaries. Finally, load capacities are assigned to buses by matching the load values to those of a real power grid by using the load and connectivity data of some IEEE test systems.

Second, using the developed model, the power grid is clustered into subnetworks using the k-means clustering algorithm and in each cluster, trees are constructed from a realization of the stochastic power grid model based on the physical links that exist between buses. The impact factor of each bus is then computed based on Katz Centrality, load capacity, and the presence of distributed energy resources (DERs). This shall be used to select buses for PMUs allocation.

Third, with a predetermined total budget that can be spent over a number of years, an allocation strategy is formulated in order to satisfy the technical threshold on observability at each year, in an expanding power grid, such that the total budget is satisfied over all the deployment years. We show that the allocation problem can be solved using a constrained finite-horizon Markov decision process (MDP) algorithm.

Fourth, the topological characteristics of the proposed power grid model are compared to Florida real power grid in

terms of bus betweenness centrality, nodal degree distribution, eigen-spread values and clustering coefficients. We show that the stochastic geometry-based model provides accurate spatial approximation to real power grids.

Fifth, the proposed metering allocation is tested for different allocation strategies on an 84-bus transmission system derived from the stochastic geometry-based smart grid model, on the standard IEEE 123-bus distribution system, and on the EPRI circuit 24 distribution test system consisting of 1355 buses².

The remainder of this paper is organized as follows. In Section II, a stochastic power grid system model is presented. Section III presents the trees construction with the calculations of the impact factors of buses. Section IV formulates the dynamic programming allocation for PMUs. Section V-A compares the features of the proposed model with a real power grid, while Section V-B presents the results for the multi-year PMUs allocation for both transmission and distribution power systems. Finally, conclusions are drawn in Section VI.

II. SPATIO-TEMPORAL POWER GRID MODEL

In this section, the development of the stochastic geometry-based power grid model is described.

Tools from stochastic geometry are used to model the overall topology of the power grid in order to obtain a statistical framework for placement of PMUs. A doubly stochastic spatio-temporal model is used where: i) iterated Poisson tessellations such as PLP is used to model the spatial locations of the irregular layout of roads [19] (since PMUs are most likely to be located on roadways which are linear and randomly oriented [3]); and ii) a homogeneous one-dimensional (1D) PPP is used to model the irregular spatial locations of buses on each road [3], [20]. We will show in Section V-A that the proposed power grid model captures the topological characteristics and statistics of real power grids in terms of bus betweenness centralities, eigen-spread values, nodal degree distribution, and bus clustering coefficients.

Let $t \in \{1, \dots, T\}$ denote unit time steps such as years. Initially, the Poissonian city is built by generating lines (i.e., roads) in a disk representing the geographical region. Then, at time step $t = 1$, buses are generated on each line, which are then connected with lines following the physical paths. Finally, random load capacities are assigned for each bus by matching the values with those of a real power grid. At subsequent time steps ($t > 1$), the grid expands as new buses and physical links are installed. A detailed step-by-step process for constructing this model is summarized in Fig. 1 and described as follows:

Step 1: Define a geographical region, such as a city, a town, etc., as a disk $\mathcal{A}(0, R)$ with radius R .

Step 2: To represent roads, a random collection of lines is generated from a set of points distributed according to a Poisson distribution on a representation space, where each line l is characterized by $0 \leq \theta_l < 2\pi$ as the line direction, and $0 < p_l \leq R$ as the line location. Let λ_l be the density of the PLP, Φ_l , in the representation space. Then, the number of lines intersecting the geographical disk is $2\pi\lambda_l R$.

²Note that the metering allocation results of the EPRI distribution system exhibited similar performance to that of the IEEE 123-bus distribution system, and thus were omitted due to space limitations.

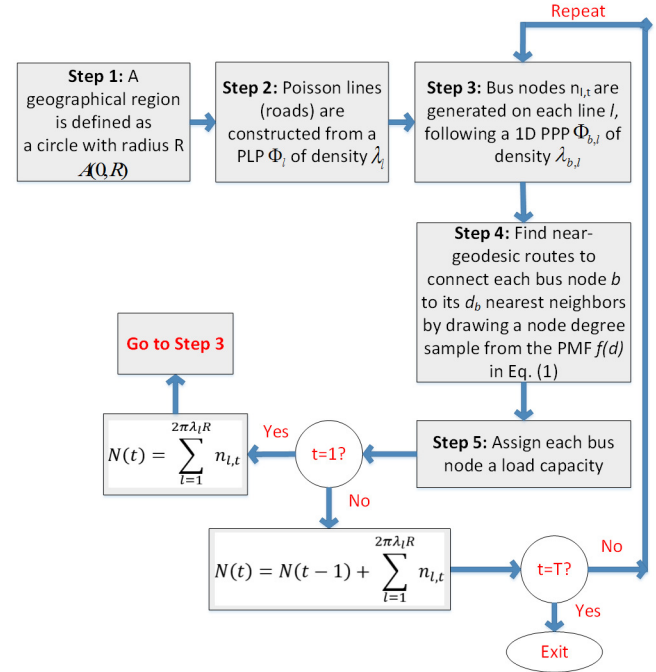


Fig. 1: A diagram summarizing the steps to obtain a generative stochastic geometry-based power grid model.

Step 3: Create buses on each Poisson line l for $l \in \Phi_l$, such that their locations are modeled following a homogeneous 1D PPP, $\Phi_{b,l}(t)$, with density $\lambda_{b,l}(t)$ for time step t . That is, all the buses in the whole power grid constitute a PPP $\Phi_b(t)$ with density being $\lambda_b(t) = \sum_{l=1}^{2\pi\lambda_l R} \lambda_{b,l}(t)$. Then, the total number of buses, $N(t)$, in the power grid can be expressed as $N(t) = \sum_{l=1}^{2\pi\lambda_l R} \lambda_{b,l}(t)|\ell|$, where $|\ell| = 2R \sin(\cos^{-1}(p_l/R))$.

Step 4: Construct power lines such that each bus b connects to its d_b nearest neighbors. A bus degree defines the number of buses directly connected to it. The nodal degree distribution, $f(d)$ with d denoting the bus degree, follows the shifted sum of exponential distributions, which was shown in [21] to provide an accurate approximation to common power distribution system structures:

$$f(d) = \sum_i \frac{\eta_i}{\mu_K} e^{-\frac{d-k_i}{\mu_K}} \mathbb{1}(d \geq k_i), \quad (1)$$

where μ_K is the average number of lines formed by a new bus and η_i are the probabilities of a bus taking different values k_i of $K(t) = \{d_{b(t)} | b(t) \in (1, \dots, N(t))\}$.

To obtain bus b 's degree, a sample, d_b , is drawn, from the nodal degree distribution $f(d)$, and then the spatial locations of its d_b neighbors are found based on the Euclidean distance. Then b is connected to its d_b neighbors based on the geographical boundaries and physical paths by selecting one of the potential near-geodesic routes, which were shown to be good approximations to true geodesics [22], [23]. Finally, the line is marked on the route selected for each of the d_b neighbors to achieve the degree of bus b . To ensure power delivery to every bus, disconnected connections are made connected based on the shortest paths between them so as to reduce power losses. Note that distribution power systems have more radial-like

network configuration structures, while transmission power systems can have multiple loops to guarantee power delivery in case of line faults or failures [24].

Step 5: Assign load values to load buses as follows. First, the aggregate load demand is obtained as [25]:

$$\log [P_L^{\text{tot}}(N_L(t))] = -0.2(\log N_L(t))^2 + 1.98 \log N_L(t) + 0.58,$$

where $N_L(t)$ is the total number of load buses at time t supporting customer demands; $P_L^{\text{tot}}(N_L(t)) = \sum_{l=1}^{2\pi\lambda_l R} P_l(t)$; and $P_l(t)$ is the aggregate demand capacity of load buses on line l at time t . Then, a random set of load capacities $[P_l(t)]_{1 \times N_L(t)}$ is generated, where 99% of generated loads follow an exponential distribution with about 1% having extremely large demands falling outside the normal range (2-3 times greater) expected by the exponential distribution [25]. Then, we check if the generated load values remain in the range of the aggregate load capacity, P_L^{tot} , by verifying that $\sum_{l=1}^{2\pi\lambda_l R} P_l(t) \leq P_L^{\text{tot}}$; if the condition is not satisfied, the load values are scaled down. At this stage, the normalized nodal degree (bus degree of each bus divided by the maximum bus degree of all buses) and normalized load value (load capacity of each bus divided by the maximum load capacity of all buses) of each bus are obtained using both the obtained randomly created values and the real values from an actual power system. The probability mass function (PMF) of the two normalized variables is then compared with the 2D-PMF of the normalized variables of a real power system, so we can match the probability values and re-order the capacities to the corresponding buses. Finally, the real (unnormalized) load values are assigned to load buses based on their nodal degree [25]. In this paper, the load and connectivity data of some IEEE test systems are used.

Fig. 2 shows a realization of the stochastic geometry-based transmission system with 84 buses.

III. TREES CONSTRUCTION AND IMPACT FACTORS OF BUSES

After a generative power grid model is constructed, we need to determine the importance of each bus for the purpose of meter allocation. If a bus has a high degree of centrality, i.e., physical connections with other buses, then this bus becomes an influential bus in terms of improving the grid state estimation. The reason is that the closer a non-observable bus is to an observable bus, the better the grid status can be inferred based on historical data. We shall identify influential buses with the highest number of connections with other buses using Katz centrality. Therefore, initially, graph trees are constructed from the physical model in order to calculate for each bus i) the impact factors related to bus' centrality, load capacity and DERs, and ii) the amount of uncertainty in the grid state estimation that can be absorbed if a PMU is placed on that bus. Note that once the number of PMUs is determined by the dynamic programming model, to be explained in Section IV, PMUs shall be placed on buses with the highest impact factors.

First, buses are clustered into different clusters using the k-means clustering algorithm. The clustering process helps ease the dynamic allocation strategy as buses closer to each other

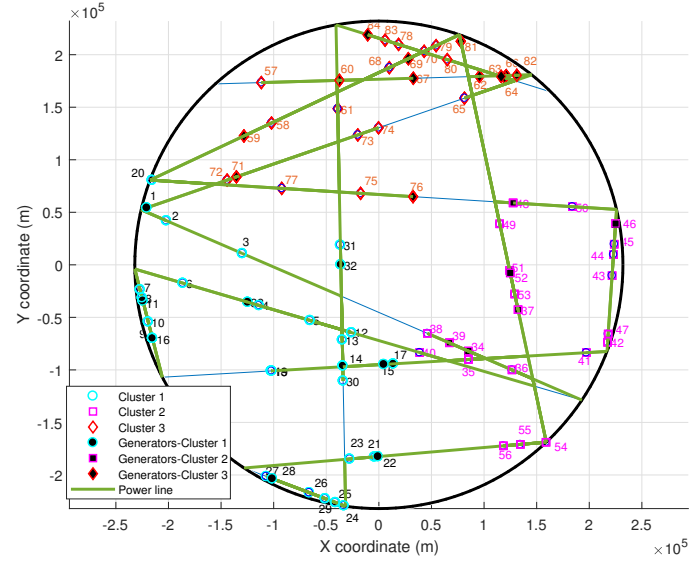


Fig. 2: An example of a realization of the stochastic geometry-based power grid model for a transmission system with 84 buses, 31 of which are randomly selected as generators, where buses are grouped into three different clusters (note that the light blue lines represent roads).

are grouped together, which helps avoid duplicate metering device installation. For each cluster, trees are constructed such that they reflect the actual physical connections between buses. Each bus is considered to be a parent bus, to which all physical connections with immediate neighboring buses are identified. Then, all other connections with non-immediate neighbors are found. All buses that lie on the identified physical lines with the respective parent bus are considered children buses. This process is repeated until all buses are covered. See Algorithm 1 for further details. It should be noted that for the distribution power systems, the trees are constructed such that they have radial structure without loops, while for the transmission power systems, the trees are constructed with multiple loops [24]. Algorithm 2 describes the process of ensuring that all buses are connected together and that cycles are removed from graph trees in the case of distribution systems.

Next, after graph trees are constructed, the impact factor of each bus is calculated based on three different criteria: i) the Katz centrality, ii) the maximum load capacity, and iii) the presence of a DER. Maximum load capacity plays a key role in determining bus importance. Monitoring becomes important when load capacity is high, since if a failure occurs, many other loads will be affected. Same holds true for a DER, as all dependent loads will be affected if a failure occurs on a DER bus node. First, the Katz centrality score, C_b , for bus b is defined as [26]

$$C_b = \beta (\mathcal{I} - \alpha_{\text{Katz}} A^T)^{-1} \vec{1}, \quad (2)$$

where A is a matrix whose elements a_{bv} denotes the $(b, v)^{\text{th}}$ element of the binary adjacency matrix $A \in \{0, 1\}^{N(t) \times N(t)}$; $\alpha_{\text{Katz}} < 1 / \max(\text{eig}(A))$ is a factor that penalizes higher order

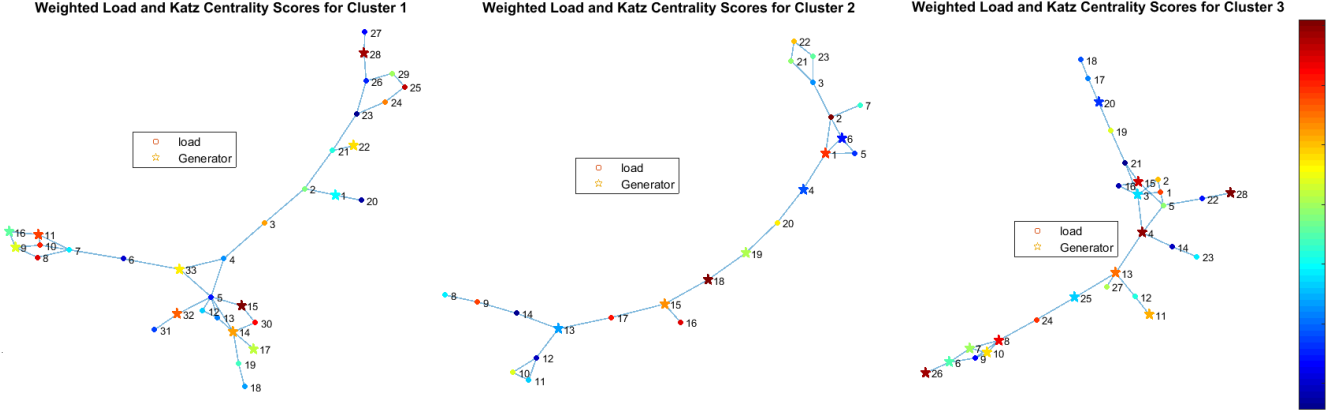


Fig. 3: Trees formation for the three clusters of the grid model of Fig. 2, with the color graph of the resulting impact factors ($w_1 = w_2 = 0.5$).

Algorithm 1 Initial graph tree construction in cluster c

Input: The topology \mathcal{T}_c of the power grid in cluster c
Output: The graph tree G_c in cluster c

- 1: Obtain children buses \mathcal{D}_b for each bus b in cluster c :
- 2:
- 3: visited buses set in cluster c : $\mathcal{V}_c \leftarrow \emptyset$
- 4: **while** \mathcal{V}_c has an unvisited bus **do**
- 5: $b :=$ an unvisited bus
- 6: visit(b)
- 7: set of children buses for bus b : $\mathcal{D}_b \leftarrow \emptyset$
- 8: $\mathcal{Y}_b \leftarrow$ set of immediate neighbors of b
- 9: **foreach** $y \in \mathcal{Y}_b$ **do**
- 10: $L_y \leftarrow$ set of y 's physical links $\in \mathcal{T}_c$ with b
- 11: $\bar{\mathcal{Y}}_b \setminus \mathcal{Y}_b \leftarrow$ set of buses lying on L_y
- 12: $\mathcal{D}_b \leftarrow \{\mathcal{Y}_b, \bar{\mathcal{Y}}_b\}$
- 13: **end for**
- 14: $\tilde{\mathcal{D}}_d \leftarrow \mathcal{D}_b$
- 15: **foreach** $d \in \tilde{\mathcal{D}}_d$ **do**
- 16: $\mathcal{Y}_d \leftarrow$ set of immediate neighbors of d
- 17: $\mathcal{D}_b \leftarrow \{\mathcal{D}_b, \mathcal{Y}_d\}$
- 18: **foreach** $y \in \mathcal{Y}_d$ **do**
- 19: $\mathcal{Y}_y \leftarrow$ set of immediate neighbors of y
- 20: $\mathcal{D}_d \leftarrow \mathcal{Y}_y$
- 21: $\mathcal{D}_b \leftarrow \{\mathcal{D}_b, \mathcal{D}_d\}$
- 22: **while** $\mathcal{D}_d \neq \emptyset$ **do**
- 23: **foreach** $d' \in \mathcal{D}_d$ **do**
- 24: $L_{d'} \leftarrow$ set of d' 's links $\in \mathcal{T}_c$ with y
- 25: $\mathcal{X} \setminus \{\mathcal{D}_b\} \leftarrow$ set of buses on $L_{d'}$
- 26: $\mathcal{Y}_{d'} \leftarrow$ immediate neighbors of d'
- 27: $\mathcal{D}_d \leftarrow \{\mathcal{X}, \mathcal{Y}_{d'}\}$
- 28: $\mathcal{D}_b \leftarrow \{\mathcal{D}_b, \mathcal{D}_d\}$
- 29: **end for**
- 30: **end while**
- 31: **end for**
- 32: **end for**
- 33: **end while**
- 34: $G_c \leftarrow \text{graph}(\{b\}, \{\mathcal{D}_b\})$

connections to measure the influence of not only the immediate bus but also the higher order bus [26]; β is a positive constant to ensure non-zero centrality; \mathcal{I} is the identity matrix; and $\vec{\mathcal{I}} = [1 \dots 1]$ is the identity vector of size $1 \times N(t)$.

Finally, the impact factor of bus b is calculated as

$$\text{IF}_b = w_1 C_b + w_2 \text{LC}_b + w_3 \text{DER}_b, \quad (3)$$

where $0 < (w_1, w_2, w_3) < 1$ are weight factors, LC_b and DER_b are the load priority value and the DER priority value, respectively, with the highest value in a cluster taking value n_c , with n_c being the number of buses in cluster c . Note that the DER priority value is only used in the distribution system.

Fig. 3 shows the trees formation for the three clusters of the grid model of Fig. 2, with the color graph indicating the resulting impact factor intensities of buses.

IV. FINITE-HORIZON DYNAMIC ALLOCATION MODEL

Here, a multi-year PMUs allocation problem is presented, whose solution is used by the power grid operator to determine the optimal number and locations of PMUs at each year. Note that while PMUs are an expensive option for distribution systems, there are some existing cases where PMUs are to be installed in a distribution system (see [27], [28], [29]).

Definition 1. (Uncertainty Absorption) Each time a PMU device is installed, it absorbs a certain amount of uncertainty in the power grid. The uncertainty in the state estimation of power grids comes from the insufficiency and inaccuracy of real-time measurements data and network parameter values. The uncertainty of the grid state can be aggravated with the penetration of distributed generation units, intermittent, unpredictable and time-varying loads, and renewable energy generation such as solar and wind energy [30]. In order to calculate the amount of uncertainty, $u_{j,t}$, that a PMU device j can absorb at time step t , we use the fraction of the j th bus degree to the degree of all of its non-allocated children buses within the cluster polygon, $\mathcal{P}(o, R_c)$, centered at o and with diameter R_c at time step t . Thus,

$$u_{j,t} = \frac{\deg(j)}{\sum_{i \in \{\{k_j^P\} \setminus \{m_{t-1}\}, j\}} \deg(i)}, \quad (4)$$

Algorithm 2 Updating graph tree structure in cluster c

Input: The graph trees G_c in cluster c

Output: Updated graph tree G_c in cluster c

```

1: Remove cycles in  $G_c$  for distribution systems:
2: if power grid is distribution system then
3:    $C_{G_c} \leftarrow$  detect all cycles in  $G_c$ 
4:   foreach cycle  $l \in C_{G_c}$  do
5:     foreach bus  $b \in l$  do
6:       longest $_b \leftarrow$  find longest physical distance to
      each  $d_b \in \{D_b \in l\}$ 
7:     end for
8:      $b^* \leftarrow \arg \max_{b \in l} (\text{longest}_b)$ 
9:     delete teh edge between  $b^*$  and  $d_{b^*}$ 
10:    end for
11:   Update  $G_c$ 
12: end if
13:
14: Ensure that all buses in  $G_c$  are connected:
15:  $\{\text{Tr}_{G_c}\} \leftarrow$  set of all tree clusters in  $G_c$ 
16: visited tree clusters set  $\mathcal{V}_{tr} \leftarrow \emptyset$ 
17: while size( $\{\text{Tr}_{G_c}\}$ ) > 1 do
18:   foreach  $tr \in \{\text{Tr}_{G_c}\}$  do
19:     foreach bus  $b \in tr$  do
20:       shortest $_b \leftarrow$  find minimum physical distance to
      each  $d_b \in \{D_b \in \{\text{Tr}_{G_c}\} / (tr, \mathcal{V}_{tr})\}$ 
21:     end for
22:      $b^* \leftarrow \arg \min_{b \in tr} (\text{shortest}_b)$ 
23:     Add a link between  $b^*$  and  $d_{b^*}$ 
24:      $\mathcal{V}_{tr} \leftarrow \{\mathcal{V}_{tr}, tr\}$ 
25:   end for
26: end while
27: Update  $G_c$ 

```

where $\deg(j)$ is the degree of bus j , $\{k_j^P\}$ is the set of the nearest neighbors to bus j within the cluster polygon P , $\{m_{t-1}\}$ is the set of buses with already allocated PMUs at time step $t - 1$.

The problem is described in the context of a dynamic programming based on the principle of optimality [31], where we define a decision variable vector x_t , a state variable vector s_t , a transition function f_t , and a cost function, c_t , corresponding to each time unit t . The dynamic problem enables us to determine at each time step the number of PMUs to allocate and their corresponding locations to satisfy budget and estimation accuracy constraints. When accurate grid estimation cannot be obtained, economic costs are incurred on the power grid operator since the cost of balancing the power generation would become higher due to the increased uncertainties in the power grid. Hence, the PMUs need to be allocated to absorb part of this uncertainty.

The decision variable at time t captured by vector $x_t = \{n_{s,t}, x_{s,t}, u_{j,t}\}$ is a tuple consisting of the number of PMUs to allocate at t , the locations of PMUs to allocate at t , and the amount of uncertainty absorbed by j^{th} PMU device at t , respectively. The state variable at time t , represented by vector $s_t = \{m_t, B_t, U_t\}$, is a tuple consisting of the number

of already allocated PMUs in the power grid until t , the state of budget at t , and the state of uncertainty of the power grid at t , respectively. The transition function, f_t , is defined by the Poisson probability density function since the number of new buses added at each time step is a Poisson random variable: $f_t = (\lambda_b^{n_{b,t}} e^{-\lambda_b}) / n_{b,t}!$, where $n_{b,t}$ is the number of buses added at time step t .

Let σ_u denotes the value of uncertainty costs related to the cost of the supplied energy to meet the demand in the case of inaccurate state estimation. The costs incurred at time t , c_t , include costs of balancing to meet the uncertainties in the demand, which is proportional to the amount of uncertainties in the power grid. The more the uncertainty is present in the power grid, the higher the costs are for purchasing energy since the system operators will have to purchase additional energy to meet their demand if needed [32], [33]. Furthermore, given a certain uncertainty level in the demand, there is an associated number of already installed PMUs (m_t), which in turn incurs labor and installation costs. In other words, the cost function can be expressed as $c_t(s_t, x_t) = \sigma_u (U_t - \sum_{j=1}^{m_t} u_{j,t}) + \sigma_c m_t$, $t \in \{1, \dots, T\}$, where $U_t - \sum_{j=1}^{m_t} u_{j,t}$ represents the remaining amount of uncertainty in the grid after m_t PMUs have been allocated at time t , and σ_c denotes the value of the labor and installation costs. Then, a linear dynamic program is formulated, where the objective is to maximize the uncertainties absorption in the power grid over a period of $1, \dots, T$:

$$\underset{n_{s,t}}{\text{maximize}} \quad \sum_t \sum_{j=1}^{n_{s,t}} u_{j,t} \quad (5)$$

$$\text{subject to} \quad \sum_t c_t(s_t, x_t) \leq B_{\text{tot}}, \quad (6)$$

$$U_t \leq D_{\text{th}}, \quad (7)$$

$$B_t > 0, \quad (8)$$

$$n_{s,t}, u_{j,t} \geq 0, \quad (9)$$

where constraint (6) ensures that the total cost over all time steps does not exceed the total available budget B_{tot} ; constraint (7) captures the condition that the uncertainty state at time t is less than or equal to the maximum allowed uncertainty D_{th} ; and constraints (8) and (9) ensure the non-negativity of the budget, number of PMUs to allocate, and the amount of absorbed uncertainty at time t .

With the above optimization problem defined, the state space at time slot t is $s(t) \in \{(m_t, B_t, U_t)\}$. Associated with this state is the amount of uncertainty absorption $\xi_t = \sum_{j=1}^{m_t} u_{j,t}$ in the same time slot. Then, the joint probability distribution of states $s^n = \{s_t\}_{t=1}^n$ and $\xi^n = \{\xi_t\}_{t=1}^n$ over n time slots can be defined as

$$\mathcal{P}(s^n, \xi^n) \stackrel{(a)}{=} \prod_{t=1}^n \mathcal{P}(s_t | s^{t-1}) \mathcal{P}(\xi_t | s_t) \quad (10)$$

$$\stackrel{(b)}{=} \prod_{t=1}^n \mathcal{P}(s_t | s_{t-1}) \mathcal{P}(\xi_t | s_t), \quad (11)$$

where s^{t-1} denotes the collection of the past $t - 1$ states; (a) comes from conditioning on the states with ξ 's being indepen-

dent of each other, i.e., $\xi^{t-1}—s_t—\xi_t$ forms a Markov chain, where ξ^{t-1} denotes the collection of the past $t-1$ uncertainties absorption; and (b) comes from the fact that the states are related in a causal and sequential manner, i.e., $s_t—s_{t-1}—s^{t-2}$ forms a Markov chain for all $t \in \{1, \dots, T\}$ [34].

Algorithm 3 Solving the Constrained Finite-Horizon MDP

Input: The time axis $\mathcal{T} = \{1, \dots, T\}$; a state space S ; a state transition matrix P ; a set of control actions $\Phi(s_t)$
Output: Optimal control policies $\mathcal{M} = \{\mu_1, \mu_2, \dots, \mu_T\}$

```

1: begin
2:   for  $t = 1 \dots T$  do
3:     foreach control action  $o(s_t) \in \Phi(s_t)$  do
4:       Define immediate reward function  $r_t = \{\xi_t(s, o) : s \in S_t, o \in \Phi(s_t)\}$ 
5:       Reward obtained:  $R_t = r_t(s_t, o_t)$ 
6:       Obtain new set of control actions  $\Phi'(s_t) = \{\Phi(s_t) : \sum_{k=1}^t R_k \geq (100 - D_{\text{Th}})\}$ 
7:       Obtain the set of control actions  $\Phi''(s_t) = \{\Phi'(s_t) : \sum_{k=1}^t o_k \leq B_{\text{tot}}\}$ 
8:     end for
9:   end for
10:  Define the optimal value function at stage  $T$  as  $V_T^*(s) = r_T(s)$ 
11:  Compute the value function  $V_k^\mu(s)$  by backward recursion [35], for  $k = \{T, \dots, 1\}$ :

$$V_k^\mu(s_k) = \{r_k(s_k, o_k) + \sum_{s' \in S_{k+1}} p_k(s'|s_k, o_k) V_{k+1}^\mu(s')\}_{o_k=\mu_k(s_k)}$$

12:  Starting with  $V_T^*(s)$ , obtain the optimal value function:

$$V_k^*(s_k) = \max_{o_k \in \Phi''(s_k)} \{r_k(s_k, o_k) + \sum_{s' \in S_{k+1}} p_k(s'|s_k, o_k) V_{k+1}^*(s')\}$$

    for  $k = \{T, \dots, 1\}$ 
13:  The optimal control policy  $\mu^*$  satisfies

$$\mu_k^*(s_k) \in \arg \max_{o_k \in \Phi''(s_k)} \{r_k(s_k, o_k) + \sum_{s' \in S_{k+1}} p_k(s'|s_k, o_k) V_{k+1}^*(s')\}$$

14: end

```

With the finite number of stages T , the constrained finite-horizon MDP is introduced in Algorithm 3 to solve the optimization problem, where the objective is to design T control policies, μ_t , that are mapped from the state space to the control space $\Phi(s_t)$, that is $\mu_t : s_t \rightarrow \Phi(s_t)$. The control state $\Phi(s_t)$ is the set of control actions taken at time step t when the system is in state s_t . The optimal control policies $\mathcal{M} = \{\mu_1, \mu_2, \dots, \mu_T\}$ are time-varying (a different optimal policy for each time step) and can be obtained by solving the recursive dynamic program backward in time from time step T to 1 [36], [37]. At each time step, we want to maximize the total expected reward (the amount of absorbed uncertainty) over all control policies, such that an optimal control policy that achieves the maximum reward is obtained. The algorithm for solving the constrained finite-horizon MDP problem is given in Algorithm 3. Once the optimal control policies are obtained, PMUs are then placed on buses starting with the bus with the highest impact factor IF_b , as given in Eq.(3), in the

first cluster, followed by the bus with the highest impact factor in the second cluster, and so on.

V. SIMULATION RESULTS AND ANALYSIS

A. Validation of the Stochastic-geometry based Power Grid

In this section, the stochastic geometry transmission system is compared with the transmission system of Florida [38] in terms of nodal degree distribution, node betweenness centrality, clustering coefficients and eigenvalues spread.

For comparison purpose, we use the MATLAB library 'MatlabBGL' provided by [39]. We use the following simulation parameters: the radius of the geographical region $R = 232$ km; the density of PLP $\lambda_l = 20$; the number of buses on each Poisson line $\text{Poiss}(\lambda_{b,l}) = 6$; the nearest neighbors $k_i = [1, 2, 3, 4, 5]$ with probabilities $\eta_i = [0.4, 0.3833, 0.1333, 0.0667, 0.0167]$; and $T = 1$ (no temporal expansion).

1) *Bus Degree Distribution:* Fig. 5 shows the PMF of the average bus degree distribution of the stochastic geometry-based power transmission system model and that of Florida. We see from Fig. 5 the similarity between both grids in terms of degree distribution, where right-skewed distribution shapes can be depicted. This justifies the use of shifted sum of exponential distributions as an accurate approximation to real power grids [21]. Fig. 4 shows the power transmission system

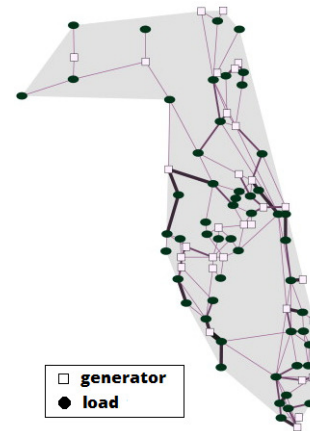


Fig. 4: Map of the power grid of Florida [38].

of Florida with 84 buses, among which 31 are generator buses. The power transmission system in Fig. 2 with 84 buses is used as a similar size stochastic geometry power grid model.

2) *Bus Betweenness Centrality:* The bus betweenness centrality is an indication of how important a bus is in terms of power flow, where the bus with the highest betweenness centrality score is the one that lies on the path of the largest number of buses [40]. This comes under the assumption that power flows over the shortest paths between buses. The complementary cumulative distribution function (CCDF) of bus betweenness centrality is plotted in Fig. 6, which depicts that only a few buses have high centrality scores since the curve is decreasing and reaches low CCDF value as the probability approaches 1. A resemblance can be noted in terms

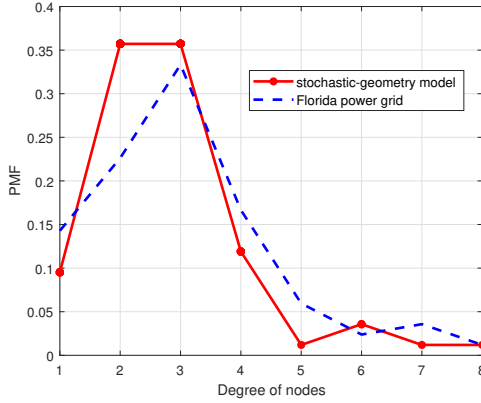


Fig. 5: Comparison between Florida's power transmission system and the stochastic geometry-based model in terms of bus degree distribution.

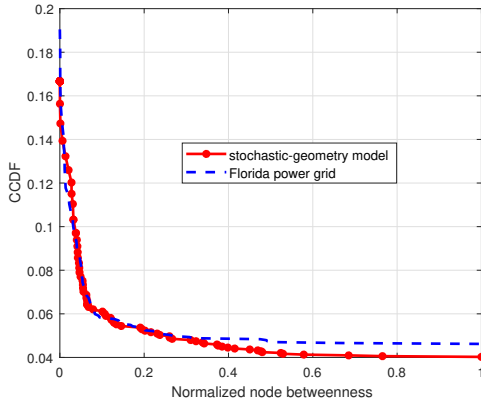


Fig. 6: Comparison of bus betweenness centrality for Florida's transmission power system and the stochastic geometry-based model.

of centrality scores between the stochastic geometry-based model and that of Florida power model.

3) *Bus Clustering Coefficients*: Bus clustering is another topological characteristic that describes clusters formation between the bus and its neighbors that have physical connections among each other. The clustering coefficient values indicate the extent to which buses tend to form clusters. Fig. 7 shows again a similarity in performance between the stochastic model and the power transmission system of Florida.

4) *Eigen-Spread Comparison*: Finally, for our last metric comparison, we look at the eigen-spread values of the power grid graph's adjacency matrix. This metric measures how well a graph is connected. A graph that maintains a good degree of connectivity is more robust to power failures, loads disconnection, topological modifications and seasonal reconfigurations. Again we see a comparable performance in Fig. 8 between the stochastic model and the power system of Florida.

5) *Similarity Scores*: To measure the similarity score between the stochastic geometry-based model and that of Florida,

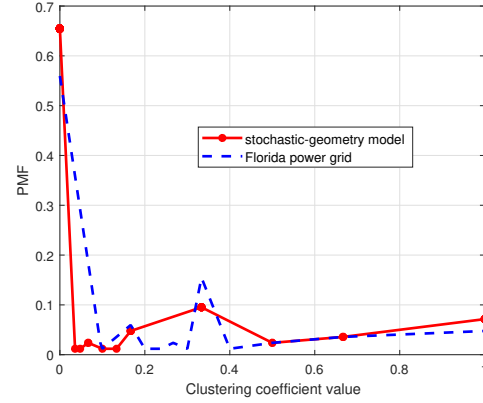


Fig. 7: Comparison of clustering coefficient between the power transmission system of Florida and the stochastic geometry-based model.

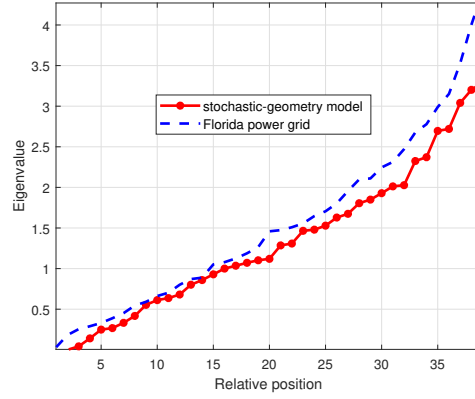


Fig. 8: Comparison of spread of eigenvalues between the power transmission system of Florida and the stochastic geometry-based model.

we use the similarity index of [41]

$$S_{f,g} = \frac{\langle f \cdot g \rangle}{\langle f \cdot f \rangle + \langle g \cdot g \rangle - \langle f \cdot g \rangle}, \quad (12)$$

where $\langle f \cdot g \rangle$ is the inner product of the functions f and g corresponding to the topological characteristics of Florida and the stochastic geometry-based model, respectively. Based on the simulation results, an average similarity score of 91.47% was found, with 96.75% for the betweenness centrality, 86.68% for the bus degree distribution, 83.42% for the clustering coefficient values, and 96.84% for the eigenvalues spread, and 93.68% for the diameter of the power grid which is a representation of the longest path connecting a pair of buses among all paths connecting any two buses. Given as an input a developed stochastic geometry-based power grid model with spatial correlation of buses and lines (that is one realization), an algorithm for the allocation of metering devices can be applied taking into consideration the geographical pattern and constraints, which would give as an output the spatial locations and installation time of PMUs.

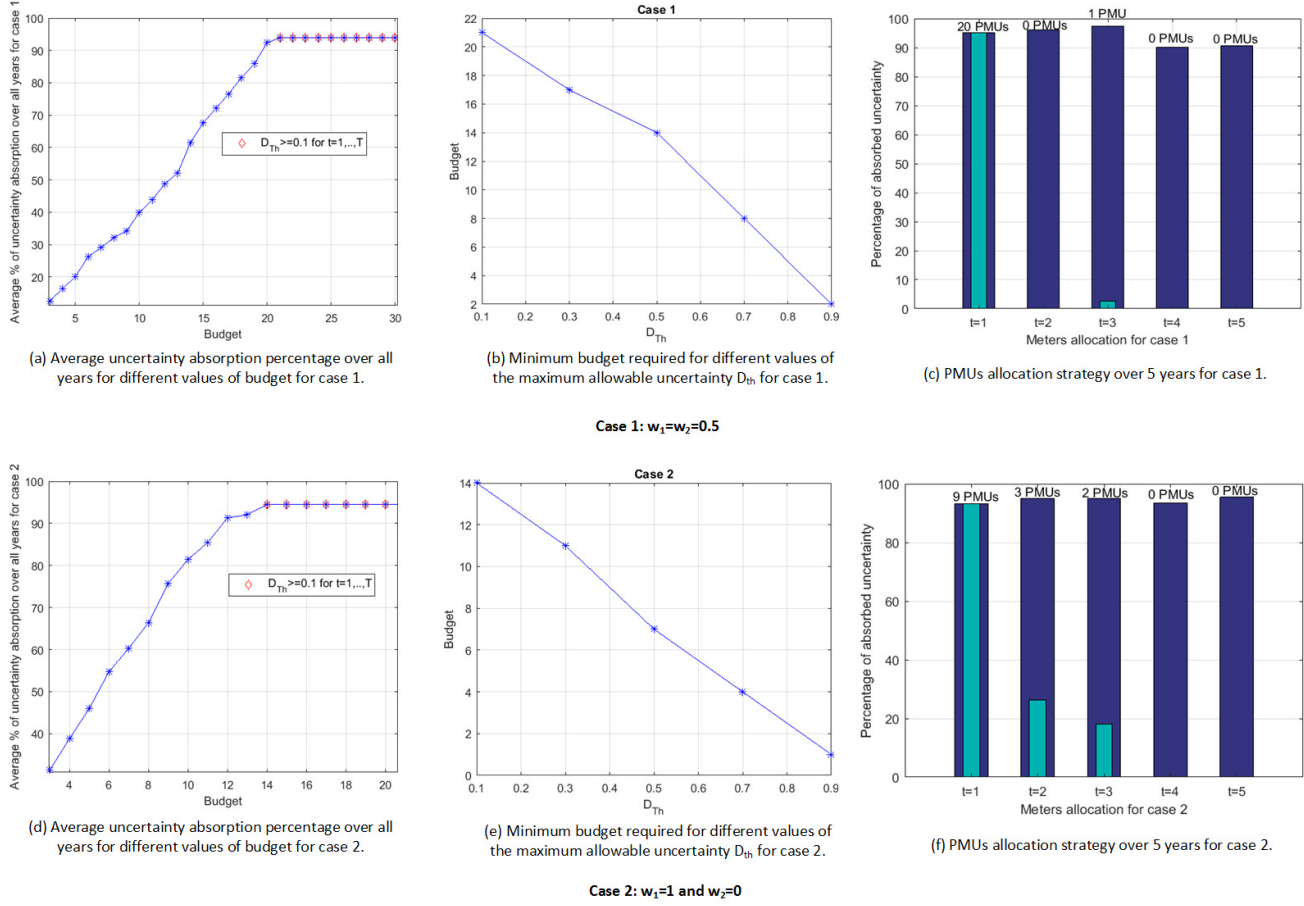


Fig. 9: Dynamic allocation results for the transmission power system of Fig. 2 for different values of weight factors.

Time Stage	Optimal locations (in bus number)
1	15, 35, 84, 28, 51, 60, 25, 49, 82, 8, 50, 71, 30, 34, 64, 10, 42, 80, 11, 48
2	-
3	37
4	-
5	-

(a) Case 1: $w_1=w_2=0.5$

Time Stage	Optimal locations (in bus number)
1	5, 34, 59, 14, 35, 60, 13, 39, 61
2	38, 36, 57
3	43, 4
4	-
5	-

(b) Case 2: $w_1=1$ and $w_2=0$

Time Stage	Optimal locations (in bus number)
1	15, 51, 84, 28, 35, 82, 25, 49, 60, 8, 50, 71, 30, 42, 64, 10, 34, 80, 11, 48
2	-
3	-
4	-
5	-

(c) Case 3: $w_1=0$ and $w_2=1$

Fig. 10: Optimal PMUs locations (in bus number) at the designated bus numbers for the transmission power system of Fig. 2 for different values of weight factors.

B. Multi-year PMUs Allocation Results

In this section, the simulation results of the multi-year PMUs allocation problem are presented using the transmission power system realization of Fig. 2. We also test the dynamic allocation policy on the standard IEEE-123 bus test system. We used the MDPtoolbox functions in MATLAB provided by [42]. For the spatio-temporal expansion of the standard IEEE 123-bus distribution power system, we used the following parameters: the number of buses on each Poisson line $\text{Poiss}(\lambda_{b,l}) = 5$; and the nearest neighbors $k_i = [1, 2, 3, 4, 5]$ with probabilities $\eta_i = [0.339, 0.339, 0.2542, 0.0424, 0.0169]$. As for the transmission power system, we used the simulation parameters of Section V-A. For both of the systems, we set the maximum allowable uncertainty, D_{th} , to 0.1. We

investigate three different cases: i) case 1 refers to taking equal weight values of the impact factors of buses, ii) case 2 refers to assigning all the weight to Katz centrality scores, and iii) case 3 refers to assigning all the weight to the load capacity values. We demonstrate the results over a period of 5 years ($T = \{1, \dots, 5\}$), where initially, it is assumed that PMUs have not been previously installed, i.e., the uncertainty percentage status of the grid is initially 100%; then, each year, new buses and lines get installed in the power grid.

The budget constraint is mapped into a fixed number of PMUs to be allocated over a period of 5 years. In each year, a variable $n_{s,t}$ PMUs get allocated, leading to a total percentage of uncertainty absorption of $u_t = \sum_{j=1}^{n_{s,t}} u_{j,t} \times 100$. Then, in subsequent years ($t > 1$), the accumulated percentage

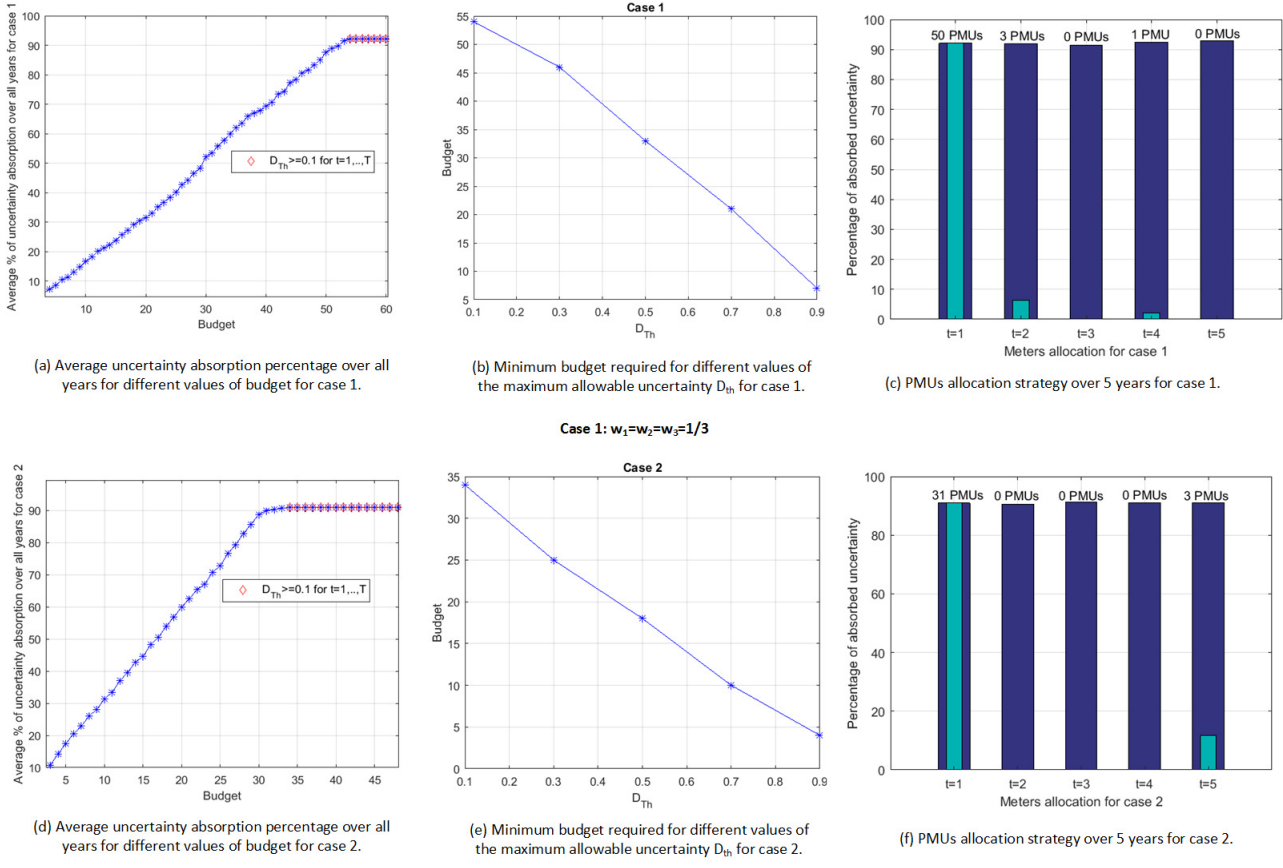


Fig. 11: Dynamic allocation results for the IEEE 123-bus distribution power system for different values of weight factors.

Time Stage	Optimal locations (in bus number)
1	47, 85, 4, 76, 16, 75, 48, 73, 49, 74, 9, 78, 58, 80, 1, 82, 29, 83, 6, 84, 11, 86, 19, 88, 20, 89, 37, 91, 22, 94, 35, 96, 24, 97, 28, 99, 43, 101, 30, 103, 33, 104, 34, 105, 50, 108, 52, 109, 53, 111
2	71, 72, 112
3	-
4	92
5	-

(a) Case 1: $w_1=w_2=w_3=1$

Time Stage	Optimal locations (in bus number)
1	18, 110, 13, 106, 8, 81, 21, 107, 64, 113, 19, 85, 23, 108, 34, 105, 68, 111, 67, 96, 7, 95, 66, 86, 60, 114, 25, 82, 42, 98, 9
2	-
3	-
4	-
5	80, 117, 116

(b) Case 2: $w_1=1$ and $w_2=w_3=0$

Time Stage	Optimal locations (in bus number)
1	48, 85, 49, 76, 47, 75, 58, 73, 1, 74, 4, 78, 6, 80, 9, 82, 11, 83, 16, 84, 19, 86, 20, 88, 22, 89, 24, 91, 28, 94, 29, 96, 30, 97, 33, 99, 34, 101, 35, 103, 37, 104, 43, 105, 50, 108, 52, 109, 53, 111
2	77, 79
3	-
4	-
5	93, 81

(c) Case 3: $w_1=w_3=0$ and $w_2=1$

Fig. 12: Optimal PMUs locations (in bus number) at the designated bus numbers for the IEEE 123-bus distribution power system for different values of weight factors.

of uncertainty absorption up to year t becomes $u_{acc,t} = \sum_{j=1}^{(m_t+n_s,t)} u_{j,t} \times 100$. In order to determine the minimum amount of budget required over the five years to achieve the target maximum allowable uncertainty threshold $D_{Th} = 0.1$ in each year, we plot in Fig. 9(a) and (d), the average percentage of uncertainty absorption over all the 5 years for different values of the budget for cases 1 and 2. As can be seen from Fig. 9(a), a total of 21 PMUs can achieve an average of 90% uncertainty absorption over all the 5 years.

In Fig. 9(b), we plot the total budget required for different values of the maximum allowable uncertainty threshold, D_{Th} .

Here, we can see that in order to achieve a target $D_{Th} = 0.1$, the total budget required should be at least 21 PMU devices, confirming the result obtained in Fig. 9(a). As the constraint D_{Th} is relaxed, the total budget can be reduced and therefore less PMU devices will need to be allocated.

Given a maximum total budget of 21 PMUs to achieve the target maximum allowable uncertainty threshold, $D_{Th} = 0.1$, the output result of the multi-year PMUs allocation for case 1 using dynamic programming is plotted in Fig. 9(c). The narrower bars inside the wider ones refer to the percentage of uncertainty absorption, u_t , corresponding to the PMUs that

get allocated in year t ; while the wider bars refer to the accumulated percentage of uncertainty absorption, $u_{\text{acc},t}$, up to year t . Since the power grid is evolving with time, more PMUs might be required to be installed at later stages. For instance, we see that at the third year, we need to install one additional PMU at its optimal location in order to meet the target maximum allowable uncertainty $D_{\text{Th}} = 0.1$. Simulation results revealed that cases 1 and 3 are similar in terms of the minimum budget required to achieve $D_{\text{Th}} = 0.1$ in each year, while in case 2, a lower budget might be required (since case 3 is very similar to case 1, it is omitted from the results). This allows us to conclude that Katz centrality is more important and more economic to be considered for metering allocation than load capacity alone or Katz centrality and load capacity together. A similar remark can be concluded from Fig. 11 for the distribution power system, where Katz centrality is more efficient to be considered for metering allocation than load capacity and DER. The optimal locations of buses for the three different allocation strategies (cases 1, 2 and 3) are provided by the corresponding bus numbers in the whole power grid for both the transmission and distribution power systems, as shown in Fig 10 and Fig. 12.

VI. CONCLUSIONS

In this paper, we have proposed a stochastic-geometry based power grid model that approximates common power grid structures, while reflecting on the physical constraints and boundaries of power grid elements, and capturing their spatial coupling in a defined geographical region. The proposed power grid model can be used as a tool for strategic planning and development, especially with its spatio-temporal evolution and expansion characteristics through time.

The suggested model was used to propose a multi-year PMUs allocation using a finite-horizon dynamic program for both transmission and distribution power systems. Given a power grid model realization, we showed how to cluster buses, construct their trees, and assign their impact factors for metering allocation purposes. This was input to the finite-horizon dynamic programming that determined the number of metering points to allocate and the amount of uncertainty absorbed at each time stage. This can be very useful for regions with a limited or no smart grid infrastructure, and which require a multi-year deployment plan for metering equipment.

ACKNOWLEDGMENT

This publication was made possible by NPRP grant # NPRP10-1223-160045 from the Qatar National Research Fund (a member of Qatar Foundation). The statements made herein are solely the responsibility of the authors.

REFERENCES

- [1] M. E. Baran, "Challenges in state estimation on distribution systems," in *Power Engineering Society Summer Meeting. Conf. Proc (Cat. No.01CH37262)*, vol. 1, July 2001, pp. 429–433 vol.1.
- [2] G. Rolim, D. Passos, I. Moraes, and C. Albuquerque, "Modelling the data aggregator positioning problem in smart grids," in *IEEE Int. Conf. on Comput. and Inform. Technol.*, Oct 2015, pp. 632–639.
- [3] S. A. R. Zaidi and M. Ghogho, "Stochastic geometric analysis of black hole attack on smart grid communication networks," in *IEEE 3rd Int. Conf. on Smart Grid Commun.*, Nov 2012, pp. 716–721.
- [4] S. Ali, K. Wu, K. Weston, and D. Marinakis, "A machine learning approach to meter placement for power quality estimation in smart grid," *IEEE Trans. Smart Grid*, vol. 7, no. 3, pp. 1552–1561, May 2016.
- [5] F. Aalamifar and L. Lampe, "Cost-efficient qos-aware data acquisition point placement for advanced metering infrastructure," *IEEE Trans. Commun.*, vol. 66, no. 12, pp. 6260–6274, Dec 2018.
- [6] G. Wang, Y. Zhao, J. Huang, and R. M. Winter, "On the data aggregation point placement in smart meter networks," in *26th Int. Conf. on Comput. Commun. and Netw. (ICCCN)*, July 2017, pp. 1–6.
- [7] M. Tavasoli *et al.*, "Optimal placement of data aggregators in smart grid on hybrid wireless and wired communication," in *IEEE Smart Energy Grid Eng. (SEGE)*, Aug 2016, pp. 332–336.
- [8] M. M. Hasan and H. T. Mouftah, "Cloud-centric collaborative security service placement for advanced metering infrastructures," *IEEE Trans. Smart Grid*, vol. 10, no. 2, pp. 1339–1348, March 2019.
- [9] T. C. Xygkis and G. N. Korres, "Optimal allocation of smart metering systems for enhanced distribution system state estimation," in *Power Syst. Comput. Conf. (PSCC)*, June 2016, pp. 1–7.
- [10] S. Teimourzadeh, F. Aminifar, and M. Shahidehpour, "Contingency-constrained optimal placement of micro-pmus and smart meters in microgrids," *IEEE Trans. Smart Grid*, vol. 10, no. 2, pp. 1889–1897, March 2019.
- [11] T. C. Xygkis and G. N. Korres, "Optimized measurement allocation for power distribution systems using mixed integer sdp," *IEEE Trans. Instrum. Meas.*, vol. 66, no. 11, pp. 2967–2976, Nov 2017.
- [12] J. Liu *et al.*, "Trade-offs in pmu deployment for state estimation in active distribution grids," *IEEE Trans. Smart Grid*, vol. 3, no. 2, pp. 915–924, June 2012.
- [13] T. C. Xygkis, G. N. Korres, and N. M. Manousakis, "Fisher information-based meter placement in distribution grids via the d-optimal experimental design," *IEEE Trans. Smart Grid*, vol. 9, no. 2, pp. 1452–1461, March 2018.
- [14] P. P. Dalawai and A. R. Abhyankar, "Placement of pmus for complete and incomplete observability using search technique," in *Annual IEEE India Conference (INDICON)*, Dec 2013, pp. 1–5.
- [15] F. Aalamifar and L. Lampe, "Optimized data acquisition point placement for an advanced metering infrastructure based on power line communication technology," *IEEE Access*, vol. 6, pp. 45 347–45 358, 2018.
- [16] Z. Wu, X. Du, W. Gu, Y. Liu, P. Ling, J. Liu, and C. Fang, "Optimal pmu placement considering load loss and relaying in distribution networks," *IEEE Access*, vol. 6, pp. 33 645–33 653, 2018.
- [17] A. A. Saleh, A. S. Adail, and A. A. Wadoud, "Optimal phasor measurement units placement for full observability of power system using improved particle swarm optimisation," *IET Generation, Transmission Distribution*, vol. 11, no. 7, pp. 1794–1800, 2017.
- [18] R. Christie, "University of washington power systems test case archive (last accessed on 25 nov 2013)(1999)," URL <http://www.ee.washington.edu/research/pstca>.
- [19] T. Courtat, C. Gloaguen, and S. Douady, "Mathematics and morphogenesis of cities: A geometrical approach," vol. 83, p. 036106, 03 2011.
- [20] Y. Jeong, J. W. Chong, H. Shin, and M. Z. Win, "Intervehicle communication: Cox-fox modeling," *IEEE J. Sel. Areas Commun.*, vol. 31, no. 9, pp. 418–433, September 2013.
- [21] D. Deka, S. Vishwanath, and R. Baldick, "Analytical models for power networks: The case of the western u.s. and ercot grids," *IEEE Trans. Smart Grid*, vol. 8, no. 6, pp. 2794–2802, Nov 2017.
- [22] W. Kendall, "Networks and poisson line patterns: fluctuation asymptotics," *Oberwolfach Reports*, vol. 5, no. 4, pp. 2670–2672, 2008.
- [23] D. J. Aldous and W. S. Kendall, "Short-length routes in low-cost networks via poisson line patterns," *Advances in Applied Probability*, vol. 40, no. 1, pp. 1–21, 2008.
- [24] D. Deka, S. Backhaus, and M. Chertkov, "Structure learning in power distribution networks," *IEEE Trans. Control of Netw. Syst.*, vol. 5, no. 3, pp. 1061–1074, Sep. 2018.
- [25] S. H. Elyas, Z. Wang, and R. J. Thomas, "On the statistical settings of generation and load in a synthetic grid modeling," *The 10th Bulk Power Systems Dynamics and Control Symposium-(IREP 2017)*, Sept 2017.
- [26] X. Wei, B. Cao, W. Shao, C. T. Lu, and P. S. Yu, "Community detection with partially observable links and node attributes," in *IEEE Int. Conf. on Big Data*, Dec 2016, pp. 773–782.
- [27] A. Tahabilder, P. K. Ghosh, S. Chatterjee, and N. Rahman, "Distribution system monitoring by using micro-pmu in graph-theoretic way," in *4th International Conference on Advances in Electrical Engineering (ICAEE)*, Sep. 2017, pp. 159–163.

- [28] A. von Meier, E. Stewart, A. McEachern, M. Andersen, and L. Mehrmanesh, "Precision micro-synchrophasors for distribution systems: A summary of applications," *IEEE Trans. Smart Grid*, vol. 8, no. 6, pp. 2926–2936, Nov 2017.
- [29] M. Farajollahi, A. Shahsavari, E. M. Stewart, and H. Mohsenian-Rad, "Locating the source of events in power distribution systems using micro-pmu data," *IEEE Trans. Power Syst.*, vol. 33, no. 6, pp. 6343–6354, Nov 2018.
- [30] D. Macii, G. Barchi, and D. Petri, "Uncertainty sensitivity analysis of wls-based grid state estimators," in *IEEE Int. Workshop on Applied Measurements for Power Syst. Proc. (AMPS)*, Sept 2014, pp. 1–6.
- [31] Y. Xu, W. Zhang, and W. Liu, "Distributed dynamic programming-based approach for economic dispatch in smart grids," *IEEE Trans. Ind. Informat.*, vol. 11, no. 1, pp. 166–175, Feb 2015.
- [32] GridWise Alliance and US DOE, "The future of the grid: Evolving to meet americas needs," *Final Report: An Industry-Driven Vision of the 2030 Grid and Recommendations for a Path Forward*, vol. 1, pp. 1–40, 2014.
- [33] M. Le Grelle, "Cost benefit analysis of smart meter deployment for residential customers, a holistic approach," Master's thesis, ETH, 2016.
- [34] L. Sankar, S. R. Rajagopalan, S. Mohajer, and S. Mohajer, "Smart meter privacy: A theoretical framework," *IEEE Trans. Smart Grid*, vol. 4, no. 2, pp. 837–846, June 2013.
- [35] D. P. Bertsekas, *Dynamic Programming and Optimal Control*, 2nd ed. Athena Scientific, 2000.
- [36] N. Bäuerle and U. Rieder, *Markov decision processes with applications to finance*. Springer Science & Business Media, 2011.
- [37] L. Kallenberg, "Finite horizon dynamic programming and linear programming," *Methods of Operations Research*, vol. 43, pp. 105–112, July 1981.
- [38] Y. Xu, A. J. Gurinkel, and P. A. Rikvold, "Architecture of the florida power grid as a complex network," *Physica A: Statistical Mechanics and its Applications*, vol. 401, pp. 130 – 140, 2014. [Online]. Available: <http://www.sciencedirect.com/science/article/pii/S0378437114000466>
- [39] D. Gleich. (2008) Matlabbbgl. Accessed on 10.14.2018. [Online]. Available: <https://www.mathworks.com/matlabcentral/fileexchange/10922-matlabbbgl>
- [40] F. Jamour, S. Skiadopoulos, and P. Kalnis, "Parallel algorithm for incremental betweenness centrality on large graphs," *IEEE Trans. Parallel Distrib. Syst.*, vol. 29, no. 3, pp. 659–672, March 2018.
- [41] R. D. Ross, *Reliability Analysis for Asset Management of Electric Power Grids*. Wiley Online Library, 2017.
- [42] I. Chades, G. Chapron, M. Cros, F. Garcia, and R. Sabbadin, "Mdptoolbox: a multi-platform toolbox to solve stochastic dynamic programming problems," *Ecography*, vol. 37, no. 9, pp. 916–920, Sept. 2014.



Rachad Atat (S'16-M'19) received the B.E. degree (with distinction) in computer engineering from the Lebanese American University (LAU), Beirut, Lebanon, in 2010, the M.Sc. degree in electrical engineering from the King Abdullah University of Science and Technology (KAUST), Thuwal, Saudi Arabia, in 2012, and the Ph.D. degree (with Hons.) in electrical engineering from the University of Kansas (KU), Lawrence, KS, USA, in 2017. He is currently a postdoctoral research associate at Texas A&M University at Qatar, working on dynamic metering allocation with integrated cybersecurity measures in smart grids. His current research interests include smart grids, cybersecurity, and Internet of Things. Dr. Atat was a recipient of the 2016 IEEE Global Communications Conference Best Paper Award, the NSF Travel Grant Award in 2016, the KU Engineering Fellowship Award, and the KAUST Discovery Scholarship Award.



Muhammad Ismail (S'10-M'13-SM'16) received the B.Sc. (Hons.) and M.Sc. degrees in electrical engineering (electronics and communications) from Ain Shams University, Cairo, Egypt, in 2007 and 2009, respectively, and the Ph.D. degree in electrical and computer engineering from the University of Waterloo, Waterloo, ON, Canada, in 2013. From 2013 to 2019, he was an Assistant Research Scientist with the Department of Electrical and Computer Engineering, Texas A&M University at Qatar. He is currently an Assistant Professor with the Department of Computer Science, Tennessee Tech. University, Cookeville, TN, USA. His research interests include smart grids, wireless networks, and cyber-physical security. He was a co-recipient of the Best Paper Awards in the IEEE ICC 2014, the IEEE Globecom 2014, the SGRE 2015, the Green 2016, and the Best Conference Paper Award from the IEEE Communications Society Technical Committee on Green Communications and Networking at the IEEE ICC 2019. He was the Workshop Co-Chair in the IEEE Greencom 2018, the TPC Co-Chair in the IEEE VTC 2017 and 2016, the Publicity and Publication Co-Chair in the CROWNCOM 2015, and the Web-Chair in the IEEE INFOCOM 2014. He is an Associate Editor for the IEEE Transactions on Green Communications and Networking, the IET Communications, and Elsevier PHYCOM. He was an Editorial Assistant of the IEEE Transactions on Vehicular Technology, from 2011 to 2013. He has been a Technical Reviewer of several IEEE conferences and journals.



Mostafa Shaaban (S'11-M'15) received the B.Sc. and M.Sc. degrees in electrical engineering from Ain Shams University, Cairo, Egypt, in 2004 and 2008, respectively, and the Ph.D. degree in electrical engineering from the University of Waterloo, Waterloo, Ontario, Canada, in 2014. Currently, he is an assistant professor in the Department of Electrical Engineering, American University in Sharjah. He is also an adjunct assistant professor in the Electrical and Computer Engineering, University of Waterloo, Waterloo, Ontario, Canada. His research interests include smart grid, renewable DG, distribution system planning, electric vehicles, storage systems, and bulk power system reliability.



Erchin Serpedin (F'13) is a professor with the Department of Electrical and Computer Engineering, Texas A&M University, College Station. He received the specialization degree in transmission and processing of information from Ecole Supérieure de l'Électricité, Paris, in 1992, the M.Sc. degree from the Georgia Institute of Technology in 1992, and the Ph.D. degree from the University of Virginia in January 1999. Dr. Serpedin is the author of two research monographs, one textbook, 17 book chapters, 160 journal papers, and 260 conference papers. His current research interests include signal processing, machine learning, cyber security, smart grids, bioinformatics, and wireless communications. He served as an associate editor for more than 12 journals and as a Technical Chair for six major conferences.



Thomas Overbye (S'87-M'92-SM'96-F'05) is a TEES Eminent Professor in the Department of Electrical and Computer Engineering at Texas A&M University (TAMU). He received his BS, MS, and Ph.D. degrees in Electrical Engineering from the University of Wisconsin-Madison. Dr. Overbye has extensive experience in many aspects of electric power systems, including participating in or leading numerous large-scale electric grid studies.